

 Open access • Journal Article • DOI:10.1016/J.JFRANKLIN.2017.11.031

Implementation of phase controlled impact device for enhancement of frequency response function in operational modal testing — [Source link](#)

Hong Cheet Lim, Zhi Chao Ong, Anders Brandt

Institutions: University of Malaya

Published on: 01 Jan 2018 - Journal of The Franklin Institute-engineering and Applied Mathematics (Pergamon Press)

Topics: Modal testing, Modal analysis, Frequency response, Modal and Phase angle

Related papers:

- [Automated impact device with non-synchronous impacts: a practical solution for modal testing during operation](#)
- [Modal Phase Compensation for Application of Direct Velocity Feedback to Active Control of Floor Vibration Under Impact Excitation](#)
- [Enhancement of Impact-synchronous Modal Analysis with number of averages](#)
- [Modal Vibration Reduction of Active Magnetic Bearings Rotor System Based on Adaptive Frequency Estimation Algorithm](#)
- [Sensor layout design procedure for active control of floor panel vibration with modal filtering technique](#)

Share this paper:    

View more about this paper here: <https://typeset.io/papers/implementation-of-phase-controlled-impact-device-for-39pw8igg5m>

Implementation of phase controlled impact device for enhancement of frequency response function in operational modal testing

Lim, H. C.; Ong, Zhi Chao; Brandt, Anders

Published in:
Journal of The Franklin Institute

DOI:
[10.1016/j.jfranklin.2017.11.031](https://doi.org/10.1016/j.jfranklin.2017.11.031)

Publication date:
2018

Document version:
Accepted manuscript

Document license:
CC BY-NC-ND

Citation for polished version (APA):
Lim, H. C., Ong, Z. C., & Brandt, A. (2018). Implementation of phase controlled impact device for enhancement of frequency response function in operational modal testing. *Journal of The Franklin Institute*, 355(1), 291-313. <https://doi.org/10.1016/j.jfranklin.2017.11.031>

Go to publication entry in University of Southern Denmark's Research Portal

Terms of use

This work is brought to you by the University of Southern Denmark.
Unless otherwise specified it has been shared according to the terms for self-archiving.
If no other license is stated, these terms apply:

- You may download this work for personal use only.
- You may not further distribute the material or use it for any profit-making activity or commercial gain
- You may freely distribute the URL identifying this open access version

If you believe that this document breaches copyright please contact us providing details and we will investigate your claim.
Please direct all enquiries to puresupport@bib.sdu.dk

Accepted Manuscript

Implementation of phase controlled impact device for enhancement of frequency response function in operational modal testing

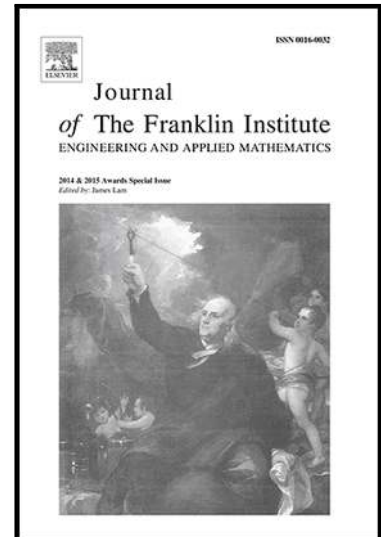
Zhi Chao Ong , H.C. Lim , A. Brandt

PII: S0016-0032(17)30617-8
DOI: [10.1016/j.jfranklin.2017.11.031](https://doi.org/10.1016/j.jfranklin.2017.11.031)
Reference: FI 3241

To appear in: *Journal of the Franklin Institute*

Received date: 26 August 2016
Revised date: 3 October 2017
Accepted date: 6 November 2017

Please cite this article as: Zhi Chao Ong , H.C. Lim , A. Brandt , Implementation of phase controlled impact device for enhancement of frequency response function in operational modal testing , *Journal of the Franklin Institute* (2017), doi: [10.1016/j.jfranklin.2017.11.031](https://doi.org/10.1016/j.jfranklin.2017.11.031)



This is a PDF file of an unedited manuscript that has been accepted for publication. As a service to our customers we are providing this early version of the manuscript. The manuscript will undergo copyediting, typesetting, and review of the resulting proof before it is published in its final form. Please note that during the production process errors may be discovered which could affect the content, and all legal disclaimers that apply to the journal pertain.

Highlights

- Phase controlled impact device replacing manual impact hammer in ISTA
- A quick and direct cancellation of dominant disturbance by using this device
- Dominant periodic response is reduced by 87%-92% with minimal averages
- A reduction of 59.03% at the second harmonic at 30 Hz is also achieved
- Improved FRF estimation and good correlation of modal extraction data with EMA

ACCEPTED MANUSCRIPT

Implementation of phase controlled impact device for enhancement of frequency response function in operational modal testing

Corresponding author

Ong Zhi Chao (Z.C. ONG)

Mechanical Engineering Department, Engineering Faculty, University of Malaya

Mailing address

Mechanical Engineering Department, Engineering Faculty, University of Malaya, 50603 Kuala Lumpur, MALAYSIA.

Phone no.

(+603) 79676815; (+6012) 4192911

Fax no.

(+603) 79675317

Email address

zhichao83@gmail.com; alexongzc@um.edu.my

Co-authors

Lim Hong Cheet (H.C. Lim)

Mechanical Engineering Department, Faculty of Engineering, University of Malaya, 50603 Kuala Lumpur, MALAYSIA (h_chet_l@siswa.um.edu.my)

Anders Brandt (A. Brandt)

Department. of Technology and Innovation, University of Southern Denmark, Campusvej 55, DK-5230 Odense M, Denmark (abra@iti.sdu.dk)

Implementation of phase controlled impact device for enhancement of frequency response function in operational modal testing

H.C. Lim

Department of Mechanical Engineering, Faculty of Engineering, University of Malaya, 50603 Kuala Lumpur, MALAYSIA (h_chet_l@siswa.um.edu.my)

Z.C. Ong

Department of Mechanical Engineering, Faculty of Engineering, University of Malaya, 50603 Kuala Lumpur, MALAYSIA (zhichao83@gmail.com, alexongzc@um.edu.my)

A. Brandt

Department of Technology and Innovation, University of Southern Denmark, Campusvej 55, DK-5230 Odense M, Denmark (abra@iti.sdu.dk)

ABSTRACT

This paper studies how to enhance frequency response function (FRF) estimation in the presence of harmonic disturbances during operational modal testing. A novel technique which utilizes impact-synchronous time averaging (ISTA) called impact-synchronous modal analysis (ISMA) was introduced where modal analysis can be performed in the presence of ambient forces. The phase angle information of the harmonic signal at the impact events is shown to be a key factor in enhancing the effectiveness of this technique. However, lack of knowledge and control of impact with respect to the phase angle of the disturbances using conventional impact hammer in ISMA has limited the effectiveness and practicality of this novel technique. A portable and automated phase controlled impact device is introduced in the effort to eliminate non-synchronous components with minimal possible impacts applied. This device makes use of the feeding phase angle information of responses from the cyclic load back to the device and imparts the impact at the correct time/phase which is always non-synchronous with respect to the phase of response from cyclic load. A reduced number of averages thereby expedite the overall modal testing procedure, an improved of FRF estimation and a good correlation of modal extraction data with benchmark data shown in this study has highlighted the advantages of ISTA using the proposed device.

Keywords Disturbances, Frequency response function, Impact-synchronous time averaging, Manual impact hammer, Phase controlled impact device

1. Introduction

To date, many machines are operating with a “run to failure” maintenance strategy where no actions are taken until machinery fails. This, in turn, raises the maintenance costs and the production losses are high. Thus, the analysis of dynamic response of a system is an important issue to understand its behaviour due to harmonic excitation especially during resonance prior to an immediate failure. Three important parameters govern the dynamic response of operating machine during resonance are; (i) the harmonic excitation frequency, (ii) the amount of damping, (iii) and the relationship between the mode shape coefficients in the excitation and the response point (1). The benefits of vibration monitoring and analysis will fulfill the demands for machines to be free of vibration problems such as imbalance, fatigue, wear, looseness and instability in the engines for prime mover, in reciprocating machines and in blade and disk vibrations on turbines.

Modal analysis was evolving for over 40 years and has been used extensively in determining, improving and optimizing the dynamic characteristics of all types of engineering structures. This approach involving the development of a mathematical model from the modal parameters extracted namely modal frequencies, modal damping and mode shape (2-5). Generally, the use of modal analysis cover a wide range of applications, such as validation, correction and updating of finite element model, active and passive vibration control, structural dynamic modification, sensitivity analysis, forced response prediction, substructure coupling, structural damage identification, etc (2, 6-9). Two widely used techniques are known as classical Experimental Modal Analysis (EMA) (10, 11) and Operational Modal Analysis (OMA). EMA describes the dynamic response of a structure through the measured inputs and outputs data. The Frequency Response Function (FRF) for a system is normally measured in controlled conditions, where the test structure is artificially excited by using a manual impact hammer or shaker driven by broadband signals, e.g., periodic chirp, pure and burst random noise, stepped- sine excitation, etc. However, classical EMA has a few limitations such as the exact boundary conditions for industrial plants are difficult to simulate in laboratory test, the measurement of FRF is difficult especially for large and complex structure, parts are tested rather than a complete operating system and a complete shutdown mode is required during the testing which is impractical especially for petrochemical plants (7, 12).

In most cases when only the output data is measurable while the actual excitation force is unknown, OMA is sought. OMA, also known as ambient vibration testing is a system identification process based solely on the output only data. It has drawn great attention in various engineering field due to many advantages; (i) the analysis procedure is fast and cheap in the absent of artificial exciter and simulation of boundary condition can be avoided, (ii) dynamic characteristics of a complete system

are measured instead of component, (iii) linearization of the system characteristics by using the broadband random excitation is possible and (iv) can be utilized for damage detection and in-situ vibration based health monitoring (7). Nevertheless, successful applications of OMA are subjected to stochastic white noise as the non-measured excitation. System identification in OMA can be difficult during field testing when the presence of harmonic excitations are close to the natural frequencies of the system (13). Also, the absent of input excitation force information does not result in scaled mode shape and subsequently the machine's sensitivity to a particular (harmonic) force cannot be predicted (14).

A novel method has been developed namely Impact-Synchronous Modal Analysis (ISMA) integrates with Impact-Synchronous Time Averaging (ISTA) that allows successful extraction of modal parameters during operation (12, 15-18). In ISTA, if the triggering is synchronized with the repetition rate of the impact, the averaging process will gradually filter out the asynchronous harmonic disturbance, i.e., cyclic load component and random noise. ISMA has the similar procedure as EMA where the information for input excitation can be measured during operation for subsequent FRF estimation, resulting in accurate modal parameter extraction. This technique has been successfully applied in determining the dynamic characteristics of operating structures and thus as a viable option for EMA and OMA.

When performing ISMA on operating structures with dominant periodic responses of cyclic loads and ambient excitation, a high number of averages are needed to eliminate the disturbances. The effect of number of averages on ISMA is proven in the previous study (16) where impacts were applied randomly on the operating structure using manual impact hammer as the phase angles information with respects is an unknown. An important finding showed that when the operating frequencies coincided with the natural modes, ISTA required a high number of averages to eliminate the disturbance in obtaining a better FRF estimation prior to dynamic characteristics identification. But, this is a time consuming and labour intensive process. Lack of knowledge and control of impact with respect to phase angle of the disturbances using conventional impact hammer in ISMA has limited the effectiveness and practicality of this novel technique. The effect of the phase angle of the disturbance with respect to the impact is found to be a key factor in enhancing the effectiveness of ISMA when performing modal testing on structures with dominant periodic responses from cyclic loads. Hence, study on the investigation of phase synchronization effect in the post processing stage was conducted. It showed that with fewer number of averages, ISTA is able to suppress the dominant periodic responses of cyclic loads thereby fasten the overall analysis procedure if the phase angle of the disturbance with respect to the impact is known (19, 20).

As far as we know, there are no similar investigations on the elimination of disturbances with minimal number of averages in the real time manner. An enhanced ISMA technique which to be used in real-time application would be novel and attractive. Therefore, the purpose of the present study is to design a portable and automated phase controlled impact device in the effort to eliminate non-synchronous components with minimal number of averages in real time by feeding the phase angle information of responses from the cyclic load back to the device. The core feature of the proposed impact device is that it utilizes the phase angle information and able to impart the impact at the correct time/phase which is always asynchronous with respect to the phase of response from cyclic load. By eliminating the undesired responses, a cleaner Frequency Response Function (FRF) estimation is able to obtain in the shortest possible time. In general, with the ability of impact phase selection and control, it is able to solve the limitations of the existing ISMA and application of this device has shed more light as compared to the conventional method.

2. Mathematical background

2.1. Effect of phase synchronization in ISTA

The effect of phase angle with respect to impact in ISTA could be described as follows. When the sinusoidal signature, i.e., $y(t) = A\sin(\omega t + \beta) = a\cos\omega t + b\sin\omega t$ is captured in blocks of time series, change in phase, β , results in changes of values a and b even though the amplitude A does not change. Performing block averaging on each triggered time block of signal will result in values of a and b diminishing to zero subsequently reducing A to zero as well. To keep a and b consistent, $y(t)$ has to start at the same point for every block captured, i.e., the phase angle, β has to be consistent (19).

2.2. Control of the impact device

The proposed impact device relates a control system that utilizes accelerometer and tachometer in phase selection of sinusoidal response due to cyclic load, and more particularly, to a reference input element for adjustment of the sinusoidal signal to substantially eliminate the response due to cyclic load component through ISTA. When the system under testing is in operation, both tachometer and accelerometer give the same frequency / running speed with a constant phase / time difference. Cross power spectrum is applied and the phase difference between tachometer speed component and cyclic load component can be obtained. The impact device is designed in such a way that it is capable to adapt the updated phase difference information in each triggered time block of signal and uses this information to control the correct timing to impart an impact based the electrical pulse signal of tachometer. Applying impact on the crest or trough or any phase position of the sinusoidal response due

to cyclic load is then possible. Tachometer pulse signal is preferable in phase position selection because it is cleaner (just an on-off state) as compared to acceleration sinusoidal signal which usually consists of random noises. In general, the control system can be divided into 2 stages.

2.2.1. Stage 1: Triggering

It is worth to mention that triggering interval, T_{trig} should lie between 2 and 12 s, particularly around 6 s. Such time range gives ample time for the test structure to restore to its initial condition after previous knock and also to give time for complete data acquisition process to take place. The triggering interval is determined by

$$T_{trig} = n \times \frac{BS}{SR} \quad (1)$$

where n is the number of time block length, BS is the block size and SR is the sampling rate.

2.2.2. Stage 2: Feedforward controller for the impact device

Fig. 1 shows the control approach of phase controlled impact device using feedforward method. The control objective is the maintenance of the impact location (process output) denoted by L_{real} very close to its set-point, and the manipulated variable is the impact timing for the impact device to impart an impact. The set-point here is the experimental impact location, e.g., crest and trough on the periodic response from cyclic load component represented by L_{exp} . The challenge is to reduce or, in the ideal case, eliminates the effect of the disturbances on the desired impact location by adjusting the impact timing of the impact device.

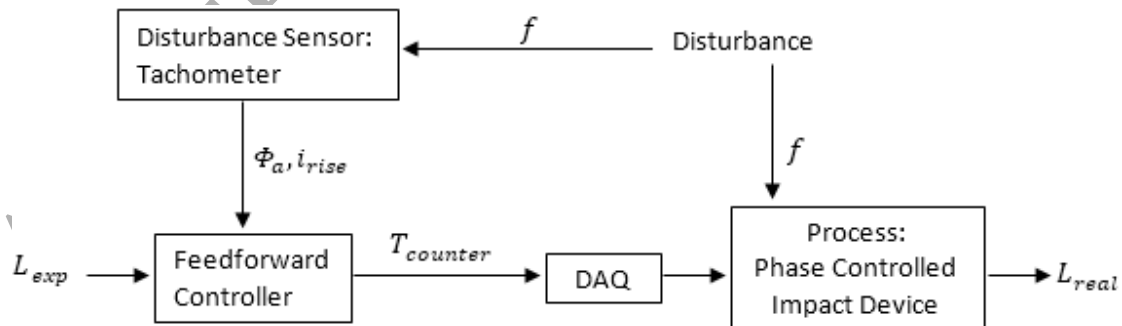


Fig. 1. Block diagram of feedforward control for phase controlled impact device. The variables indicated are the set-point, L_{exp} ; the control signal, $T_{counter}$; the process output, L_{real} ; the measured input disturbance, f .

The performance of the phase controlled impact device is directly affected by the input disturbance which is the operating frequency of a system, f , where in an ideal case, its performance is the best at constant operating frequency. However, when dealing with actual operating machinery, the measured f may vary slightly over time and sufficient to disturb the accuracy of the impact device. For incorporating such uncertainties in f , feedforward control is implemented adapting real time f from the structures at each triggered time block of signal by using tachometer.

Parameters for controlling the impact device are known as phase difference (degree), Φ_a , and array index of rising edge, i_{rise} , which can be derived from measured tachometer pulse signal. With these information, i.e., f , Φ_a and i_{rise} , one can computed the phase difference time, T_ϕ , time interval of load cycles, T_{cycle} which is the time corresponding number of load cycles added (n), time interval of desired impact, $T_{desired}$ and lag time, T_{lag} . T_{lag} is introduced defining the time interval between the last rising edge of the tachometer speed component and the end of time block right after the impact is triggered. Thus, the governing equations are given by

$$T_\phi = \left[-\frac{\Phi_a}{360^\circ} \right] \times \frac{1}{f} \quad (2)$$

$$T_{cycle} = n \times \frac{1}{f} \quad (3)$$

$$T_{desired} = \left[-\frac{\Phi_p}{360^\circ} \right] \times \frac{1}{f} \quad (4)$$

where Φ_p is the desired impact phase angle and

$$T_{lag} = [S_{ext} + S_{comp} - i_{rise}] \times \frac{1}{SR} \quad (5)$$

where S_{ext} is the extracted samples from the end of time block, S_{comp} is the compensate sample (value of 1), and i_{rise} is the array index of rising edge. The compensate sample is added to the equation as the phase difference time is calculated from the center of the tachometer speed component. Note that the time range of extracted samples must greater than period of running frequency so that at least one peak of tachometer speed component is observable in the extracted sample.

Before implementing the phase controlled impact device into the real test, it is important to take into consideration time delay taken by the impact device to impart on the surface of structure after “on”

signal is sent to the device. It is determined through dummy impacts prior to the actual counted impacts and defined as $T_{offset} = t_{real} - t_{exp}$ where t_{exp} is the experimental impact time before offset adjustment and t_{real} is the real impact time observed in response signal. Thus, the actual counter time, $T_{counter}$, forward to the controller consist of data acquisition system (DAQ) which in turns initiate an excitation signal for the impact device to impart an impact can be calculated by

$$T_{counter} = T_{\phi} + T_{cycle} + T_{desired} - T_{lag} - T_{offset} \quad (6)$$

It is noted that $T_{counter}$, T_{ϕ} , T_{cycle} , $T_{desired}$, T_{lag} and T_{offset} represent specific intervals of time whereas t_{real} and t_{exp} represent specific moments of time.

3. Measurement procedures and instrumentation

The study aims to fill the gap and limitation of current ISMA technique which requires manually operated impact hammer to excite the system under testing during operational modal testing. For that, phase controlled impact device was introduced in this study as a replacement device for traditional impact hammer in the effort to expedite the modal testing procedure while reducing disturbances with minimal averages. Hence, the only logical way of approaching this problem is to ensure that the FRFs estimation obtained using this phase controlled impact device must not only show excellent suppression of disturbances when comparing with FRFs estimation using manual impact hammer during operating conditions, but also subsequent modal parameters obtained must exhibits well correlation with benchmark EMA results.

3.1. FRF estimation using manual impact hammer

Fig. 2 presents a diagram of the experimental set-up. The main structure consists of a motor coupled to rotor shaft system where the operating frequency of the motor was set at 20 Hz and 30 Hz. In this experiment, a roving tri-axial accelerometer was used while manual impact hammer as excitation at fixed degree of freedom, i.e., point 1 in vertical direction, (i.e. z-axis). The tri-axial accelerometer was roved from point 1 to point 20 measuring the responses of the structure in axial, horizontal and vertical directions, (i.e. x-, y- and z-axis) and this gave a single-input, single-output (SISO) analysis. The number of averages was set at; (1) 10 for non-rotating condition and 20 Hz and (2) 20 for non-rotating condition and 30 Hz, respectively. Both the excitation and response signal were sent to the data acquisition hardware consisting of National Instrument NI-USB-9234 with a signal processing software, LabVIEW. Sampling rate used was 2048 samples/sec, and the vibration signal was collected for 2 seconds, so a total of 4096 samples were recorded for post-processing. Me'scope software was used to draw the

three-dimensional structural model of the test rig in coordinate points where every point was connected by straight lines as shown in Fig. 3, and also for modal parameter extraction. Table 1 shows the descriptions of the instrumentations used in this study.

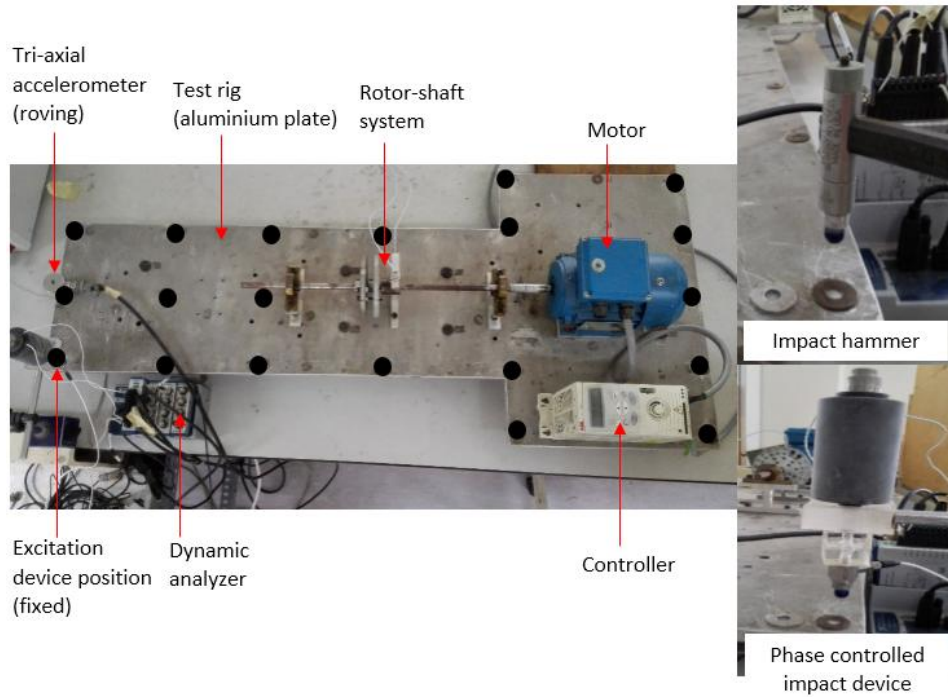


Fig. 2. Measurement locations of motor driven test rig.

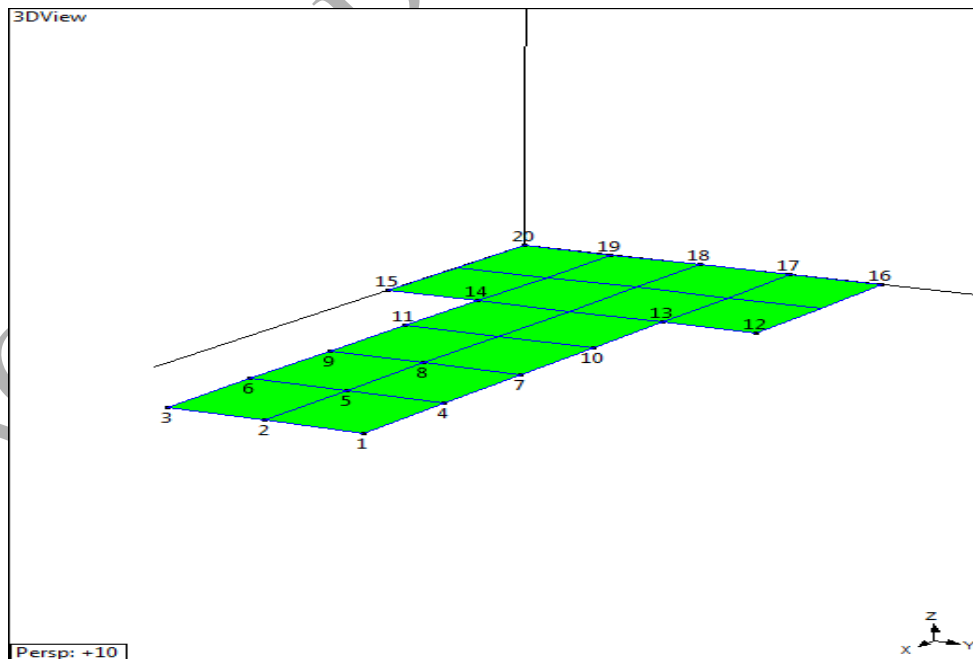


Fig. 3. Structural model of the fault simulation rig.

Table 1

List of instrumentation.

Instruments	Details
UM simulation rig	Used as a test rig to perform ISTA
PCB impact hammer (Model 086C03)	Sensitivity: 2.16 mv/N Tip type: medium tip with vinyl cover Hammer mass: 0.16 kg Frequency range: 8 kHz Amplitude range: ± 2200 N peak Impact Period: random
Phase controlled impact device and impact forcing sensor (Model 208C04)	Clamped with retort stand. Connected to channel 1 of National Instrument dynamic analysers Sensitivity: 1.162 mv/N Tip type: medium tip with vinyl cover
IMI tri-axial accelerometer (Model 604B31)	Sensitivity: 100 mv/g Frequency range: 0.5 – 5000 Hz Amplitude range: ± 50 g peak
NI USB dynamic signal acquisition module, (Model NI-USB 9234)	Number of channels: 4 ACD resolution: 24 bits Minimum data rate: 1650 samples/sec Maximum data rate: 51200 samples/sec
LabVIEW 2013	Sampling rate: 2048 samples/sec Block size: 4096 samples Channel 1: Manual impact hammer / phase controlled impact device Channel 2: Tachometer (X-axis) Channel 3: Accelerometer (Y-axis) Channel 4: Accelerometer (Z-axis) Application of exponential window in time response. Adjustment was made in Pre-Setting mode.
ME'Scope v4.0	To process FRF obtained through LabVIEW. Curve fitting is done using orthopolynomial method to extract damped natural frequency, modal damping and residue mode shape.

3.2. FRF estimation using phase controlled impact device

The experiment setups are generally the same as that of conventional EMA except on the tool it used where manual impact hammer was replaced by phase controlled impact device. This can overcome two shortfalls, i.e., impacts were excited at the same pre-defined location and the force levels were more

consistent. The ideal distance between impact tip and test rig was determined by energising the phase controlled impact device right at the moment before the impact tip makes contact with the surface of the test rig under test. Parameters that governed the control of the phase controlled impact device were T_{trig} , n , S_{ext} , S_{comp} and Φ_p . Note that the values for T_ϕ , T_{lag} and T_{offset} were different for every time block captured. The accuracy of phase controlled impact device to knock at the desired impact location on the cyclic load component before and after offset adjustment was first investigated prior to performing modal testing using this impact device. Responses due to impact at crest and trough of the cyclic load component were expected at the end of the investigation. During the modal testing, Φ_p between impacts was set at 180° for 20 Hz and 90° for 30 Hz. The ideal combination of the parameters to be set into the DAQ were tabulated in Table 2. Subsequently, 10 and 20 averages were made for 20 Hz and 30 Hz and this resulted in the direct cancellation of the disturbances leaving behind only the responses due to impact. This could also differentiate the effectiveness of using the phase controlled impact device over the manual impact hammer with lesser number of averages in FRF estimation and modal parameter extraction.

Table 2

Summary of input parameters for phase controlled impact device.

Input signal to DAQ		20 Hz	30 Hz
Triggering interval	(T_{trig})	12 sec	12 sec
Number of time block length	(n)	11 cycles	6 cycles
Extracted samples from the end of time block	(S_{ext})	105 samples	69 samples
Compensate sample	(S_{comp})	1 sample	1 sample
Desired phase angle	(Φ_p)	0° and 180°	0° , 90° , 180° and 270°

4. Results and discussion

4.1. Accuracy of phase controlled impact device

Figs. 4-7 depict four out of six responses due to impact before offset adjustment. The time intervals for $T_{counter}$, T_ϕ , T_{cycle} , $T_{desired}$, T_{lag} and T_{offset} are indicated in the figures. Ideally, the accuracy of phase controlled impact device is proven if and only if the impact location, i.e., L_{real} equals to L_{exp} from the qualitatively point of view. Besides, for ease of investigating the accuracy, it is more convenient to quantitatively compared the results of impact time, i.e., t_{exp} and t_{real} . In other words, comparison between L_{exp} and L_{real} can be represented by the difference between t_{exp} and t_{real} , respectively. For example, a value near 0 indicates that L_{exp} and L_{real} are consistent.

As seen, L_{exp} and L_{real} are not at the same position where the response due to impacts tend to happen at L_{real} instead of L_{exp} . Also, it is noted that t_{exp} is not equivalent to t_{real} in this context when T_{offset} is not taken into consideration when computing $T_{counter}$. Therefore, an averaged offset time, T_{offset} of 0.085928 s is calculated through 6 dummy impacts prior to the actual counted impacts as tabulated in Table 3. This time delay is suspected to be caused by the time travel of the tip of phase controlled impact device from resting position to surface of structure.

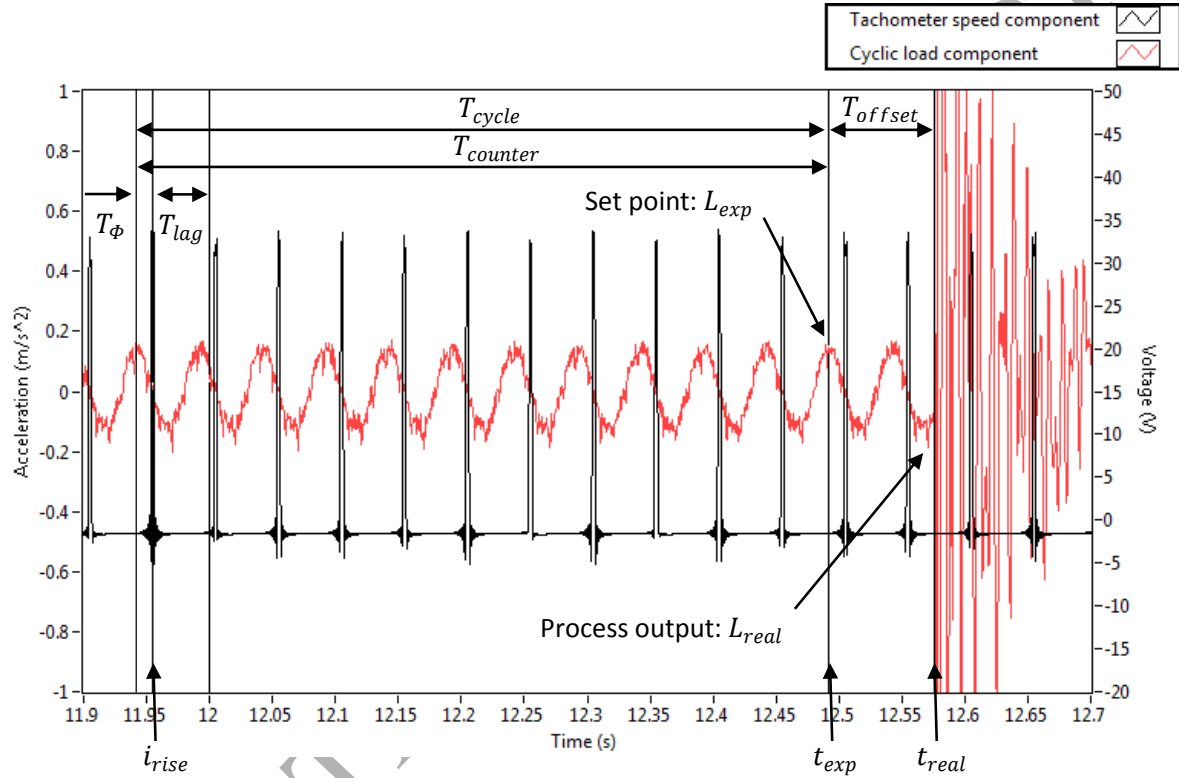


Fig. 4. First response due to impact at crest before offset adjustment.

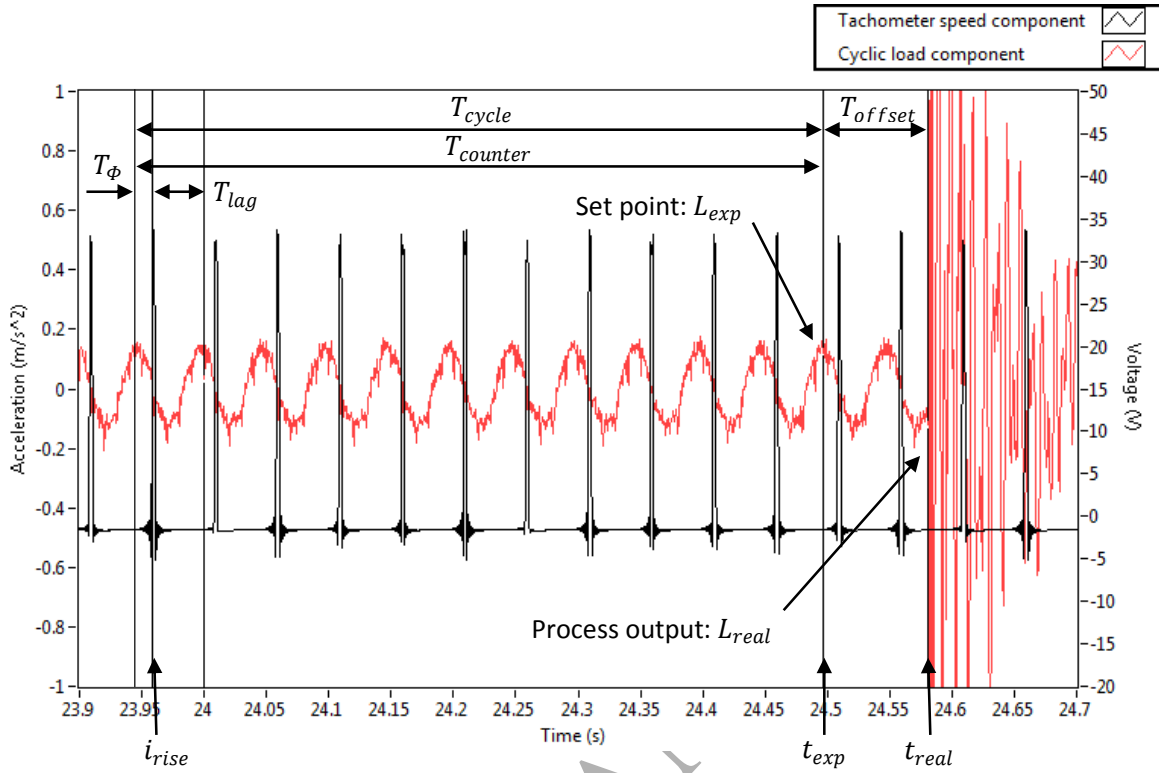


Fig. 5. Second response due to impact at crest before offset adjustment.

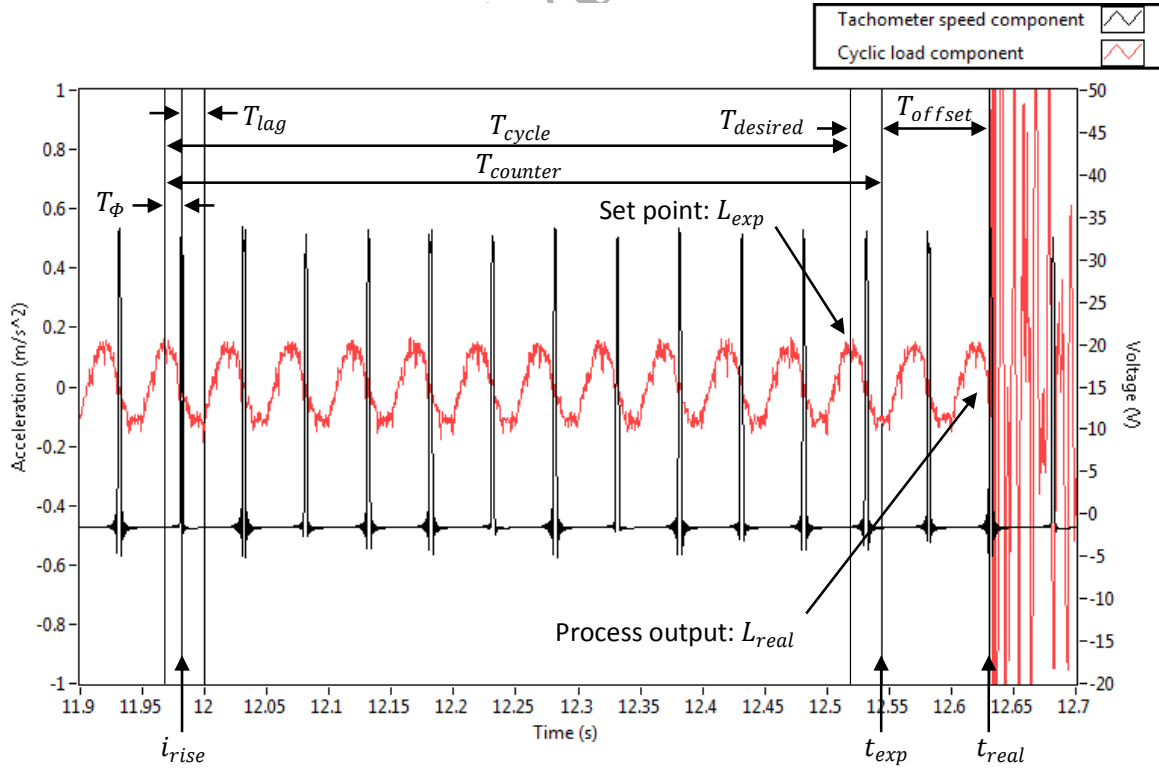


Fig. 6. First response due to impact at trough before offset adjustment.

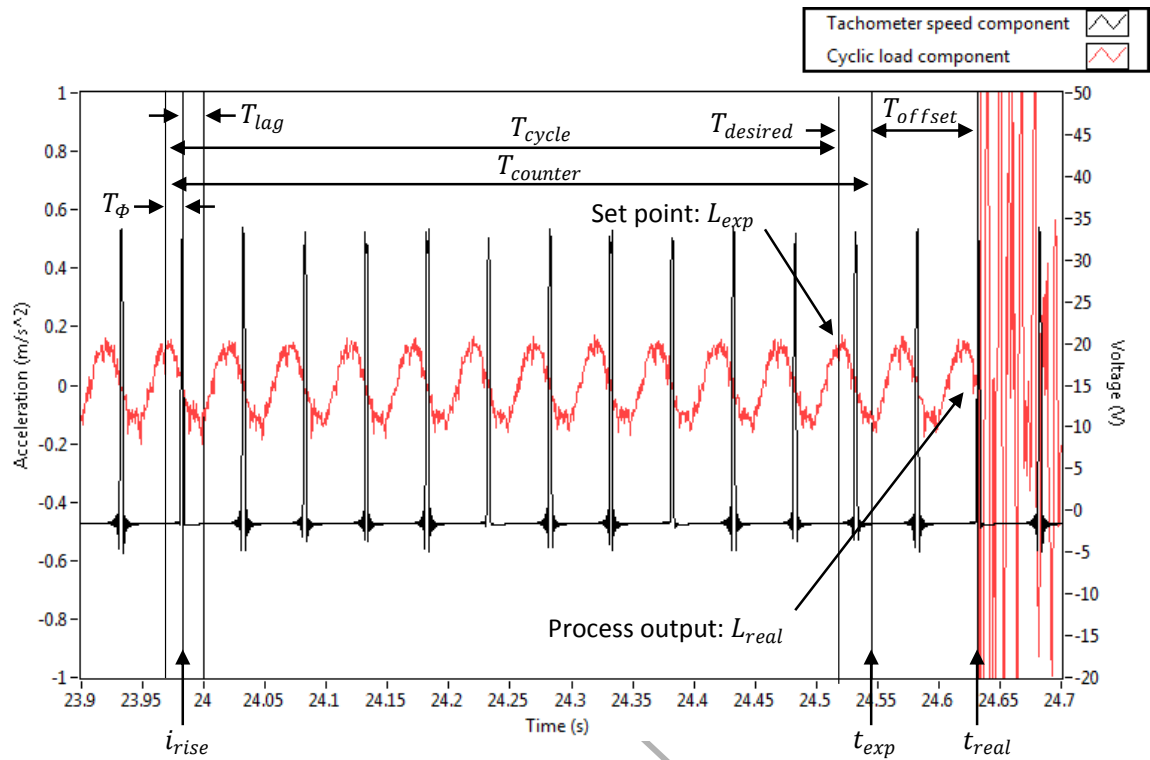


Fig. 7. Second response due to impact at trough before offset adjustment.

Table 3

Responses due to impact summary before offset adjustment.

Impact	t_{exp} (s)	t_{real} (s)	$T_{offset} = t_{real} - t_{exp}$ (s)
1	12.492147	12.575195	0.083048
2	24.496612	24.580566	0.083954
3	36.498765	36.584473	0.085708
4	12.543946	12.631836	0.087890
5	24.544711	24.631348	0.086637
6	36.543506	36.631836	0.088330
Averaged			0.085928

Figs. 8-11 show four out of six responses due to impact after offset adjustment. The latter has shown improvement where responses due to impact are as expected to occur at the crest and trough of the cyclic load component shown by L_{real} and L_{exp} . It is worth noticing that the results have been greatly improved where t_{real} are almost equal to t_{exp} as shown in Table 4 and this has suggested that the L_{real} is very close to the set-point, L_{exp} . Thus, offset adjustment plays an important role for the impact device to impact at desired impact location on the cyclic load component.

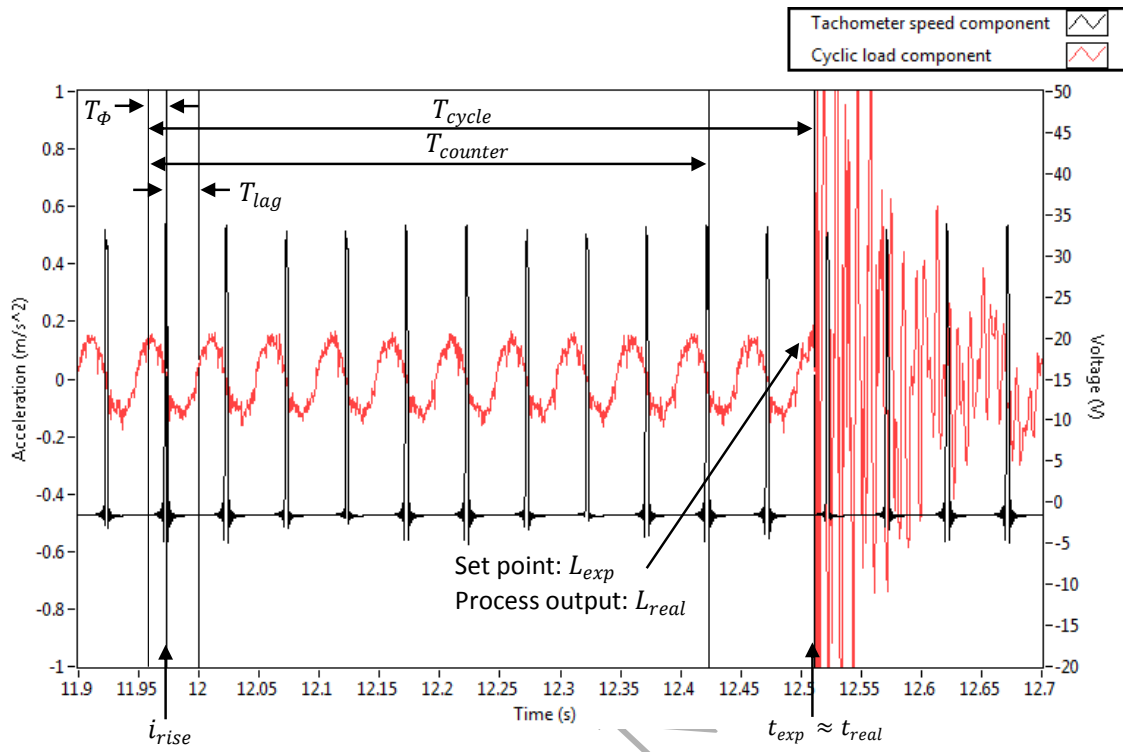


Fig. 8. First response due to impact at crest after offset adjustment.

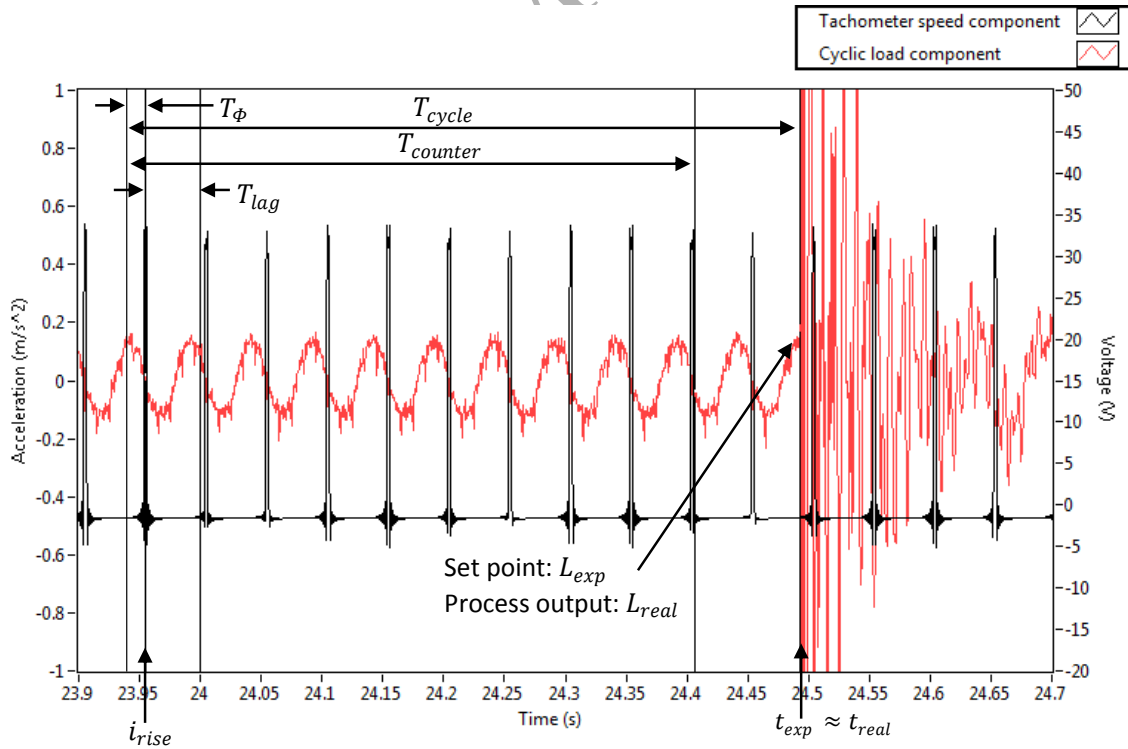


Fig. 9. Second response due to impact at crest after offset adjustment.

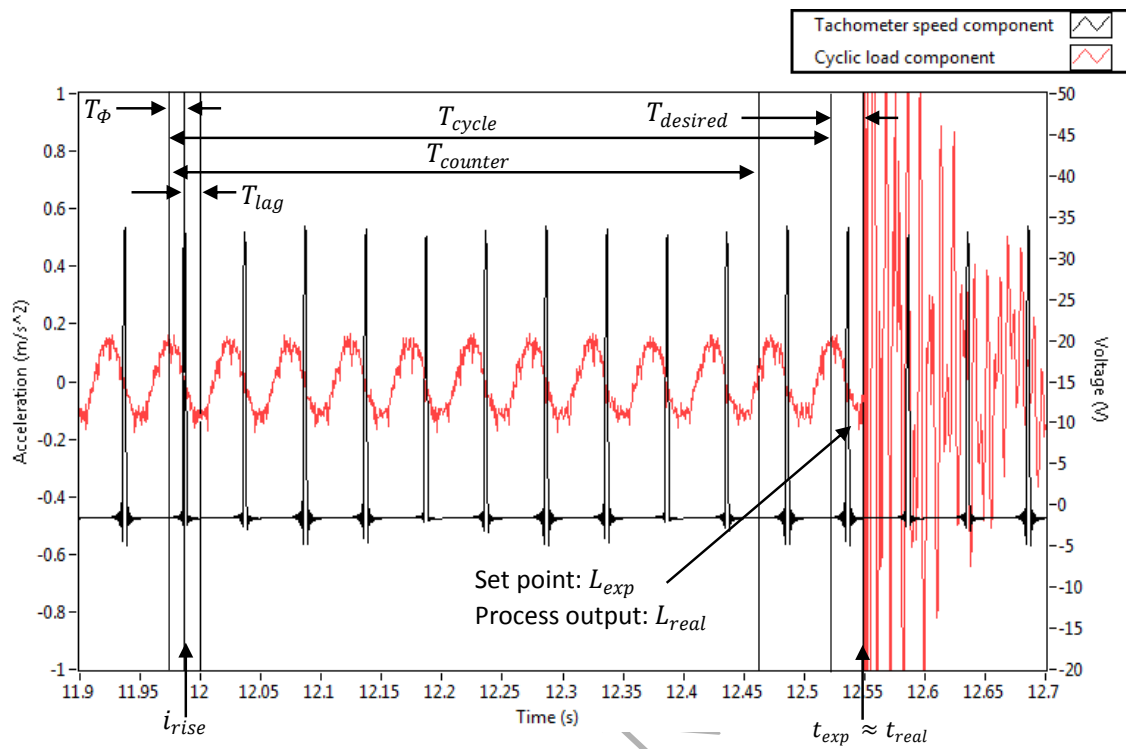


Fig. 10. First response due to impact at trough after offset adjustment.

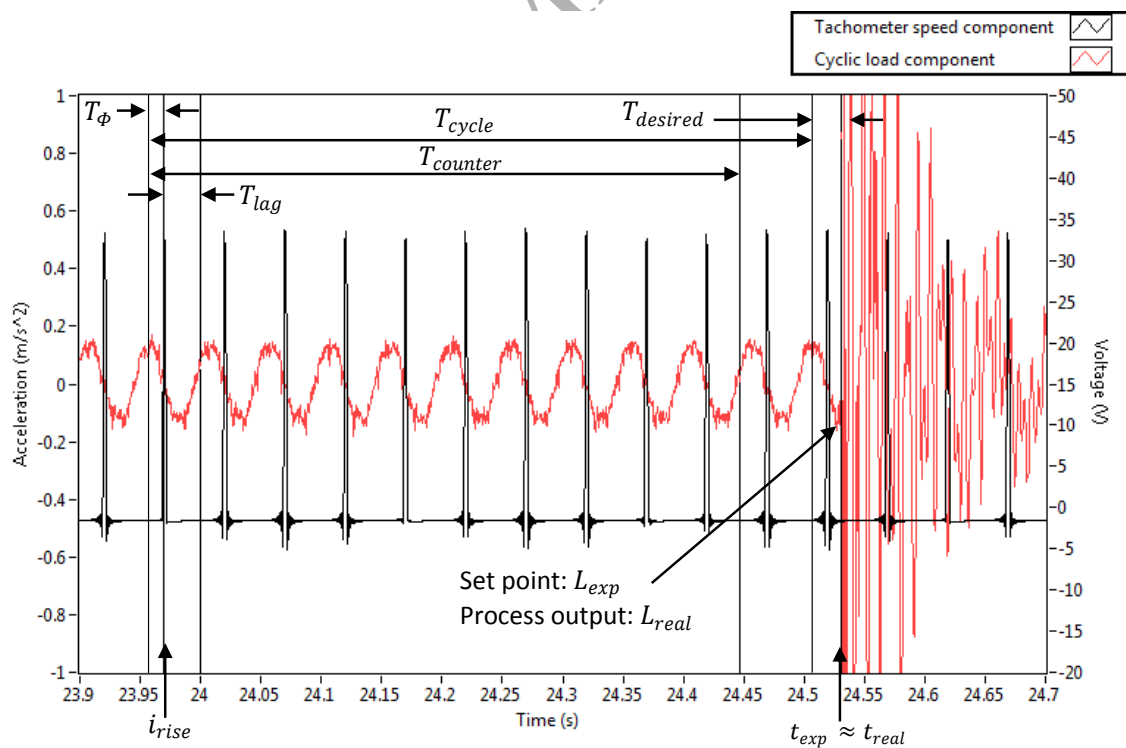


Fig. 11. Second response due to impact at trough after offset adjustment.

Table 4

Responses due to impact summary after offset adjustment.

Impact	t_{exp} (s)	t_{real} (s)	$t_{real} - t_{exp}$ (s)
1	12.509141	12.510742	0.001601
2	24.491389	24.493164	0.001775
3	36.522669	36.524902	0.002233
4	12.547776	12.549316	0.001540
5	24.531599	24.530273	-0.001326
6	36.512740	36.512695	-0.000045

4.2. Comparison of FRFs estimation

In this section, the FRFs estimation using two different excitation strategies, i.e., manual impact hammer and phase controlled impact device, for 20 Hz and 30 Hz is compared.

4.2.1. Running speed: 20 Hz

A more common scenario obtained when performing modal testing using a manual impact hammer on an operating system is presented in Fig. 12. A better FRF estimation should be free of measurement noise and leakage error. However, a highest peak originated from the cyclic load component is observed at 20 Hz with a value of $2.06 \text{ m/s}^2\text{N}$. The peak is dominant and covers up the adjacent mode subsequently a poor FRF estimation is obtained. The presence of the dominant cyclic load component in the FRF estimation using the manual impact hammer is possibly due to any of three reasons; (i) inconsistency in input force levels; (ii) inconsistency in excitation location between the impacts, and (iii) inefficient removal of the harmonic components when the impact instants are random. For modal testing using manual impact hammer, the input force levels may vary between impacts. Problem can be developed over time when the uncontrollable impact force levels are much lower than the cyclic force originated from the cyclic load component. Thus, sufficient amount of impact force is very important to dominate the total response generated by impacts and to filter out the disturbances. Besides, the user may perform the excitation at locations which slightly deviate from the predefined location. Moreover, it is worth mentioning that although the possibility that a synchronization occurs between the response due to impact and the response due to cyclic load is small, it is not totally impossible in modal testing using an impact hammer (19).

Using phase controlled impact device as the excitation device tends to overcome some of the limitations faced by using manual impact hammer in modal testing. The excitation has a consistent impact force level which stays relatively constant as the input force is well controlled by supplying constant voltage to the impact device and setting the same optimum distance between impact tip and operating structure. This will assure each impact has force level higher than the cyclic force in order to excite the natural mode of the system. Besides, the phase controlled impact device is isolated and clamped firmly by the retort stand in the horizontal position, and thus it is able to consistently impart the impacts at the predefined location in z-axis. Fig. 13 shows the FRF estimation using phase controlled impact device. It can be noted that the dominant cyclic load component has been significantly reduced during ISTA with 10 averages compared to using a manual impact hammer. The highest peak recorded a value of $0.248 \text{ m/s}^2\text{N}$. The reduction is considerably successful and the percentage of reduction is high, i.e., 87.96%. Phase controlled impact device utilizes the phase angle information from responses due to cyclic load component and imparts 10 impacts at a phase difference of 180° on the operating system. This produces five pairs of responses at the crest and trough of the cyclic load component. Since the total responses captured are at a phase difference of 180° between each impact, the signature responses due to impact are preserved while the disturbances are cancelling each other out during ISTA. Thus, the adjacent modes appear and are enhanced significantly. It is worth mentioning that the modal testing using phase controlled impact device only requires half amount of averages compared to using manual impact hammer and the reduction of dominant response from cyclic load component is significant. This is, in fact, more effective and time-saving in enhancing ISTA if the information of phase angles with respect to impact is known and utilized.

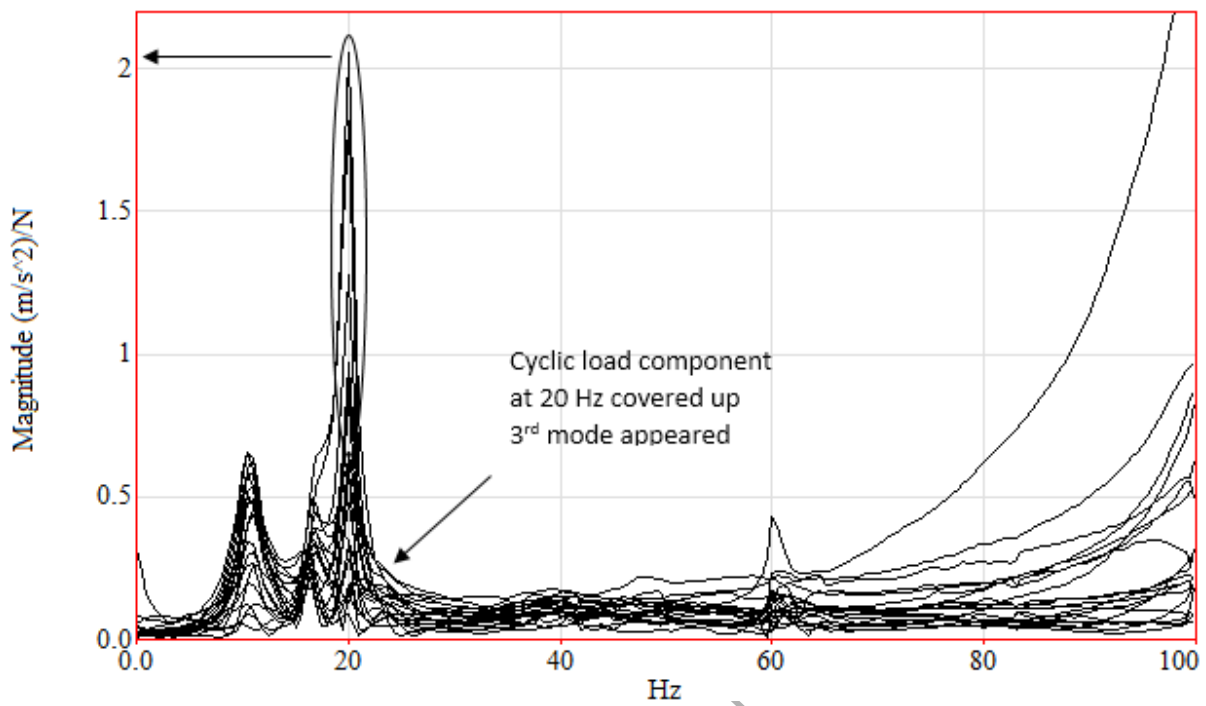


Fig. 12. FRFs estimation using manual impact hammer for 20 Hz.

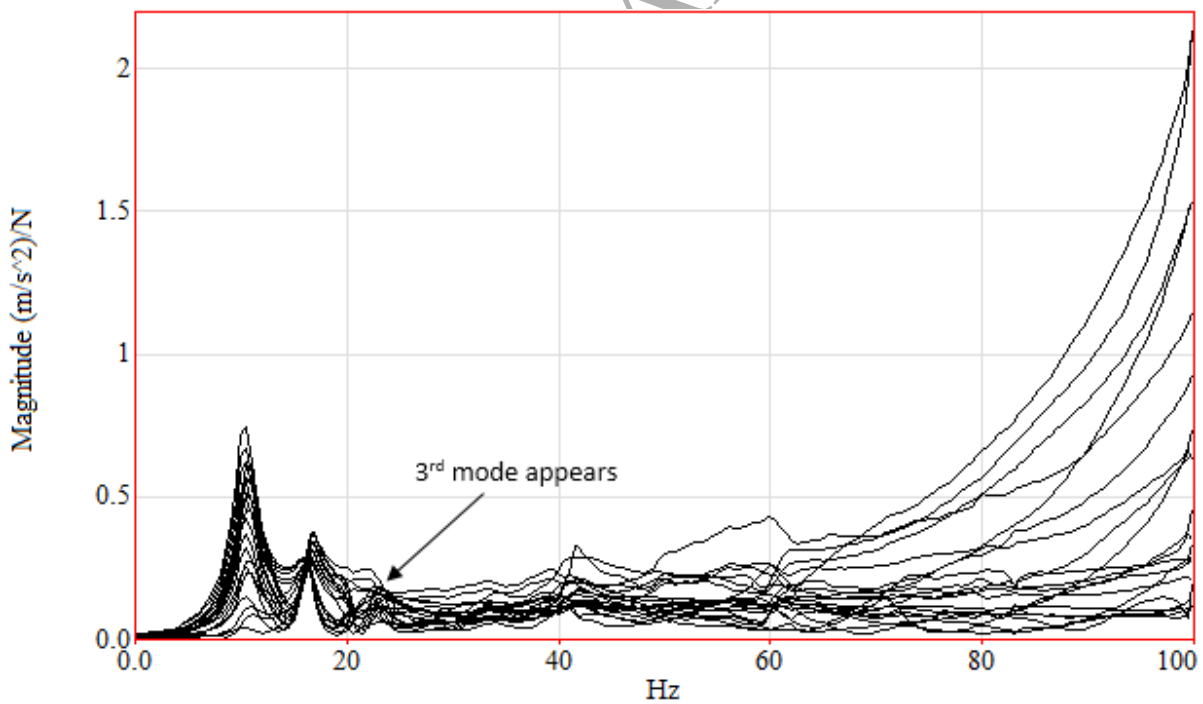


Fig. 13. FRFs estimation using phase controlled impact device for 20 Hz.

4.2.2. Running speed: 30 Hz

Fig. 14 shows the FRF estimation for ISTA using manual impact hammer. At 30 Hz, the vibration increases because of higher rotational or imbalance force. As can be seen, there are two dominant peaks originated from the cyclic load component at 30 Hz and its second harmonic at 60 Hz. The magnitude of peaks at 30 Hz and 60 Hz are identified as $2 \text{ m/s}^2\text{N}$ and $0.62 \text{ m/s}^2\text{N}$. The reasons for this phenomenon are as discussed in Section 4.2.1. In order to eliminate the disturbances, the phase controlled impact device is set to impart each impact at a phase difference of 90° . This is proven in Fig. 15 where the peak contributed by the cyclic load component and its second harmonic are significantly removed. The magnitude of peaks is reduced to $0.167 \text{ m/s}^2\text{N}$ and $0.254 \text{ m/s}^2\text{N}$. The percentage of reduction is determined as 91.65% and 59.03%. Also, successful elimination of disturbances has led to the appearance of third natural mode.

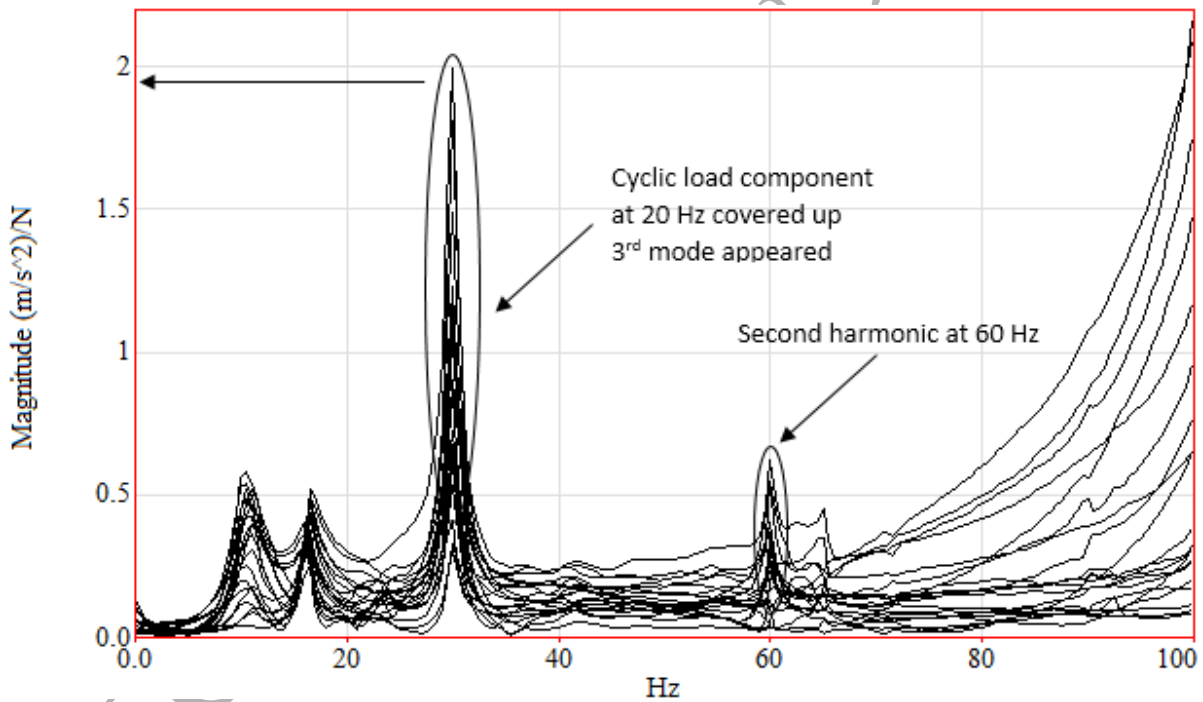


Fig. 14. FRFs estimation using manual impact hammer for 30 Hz.

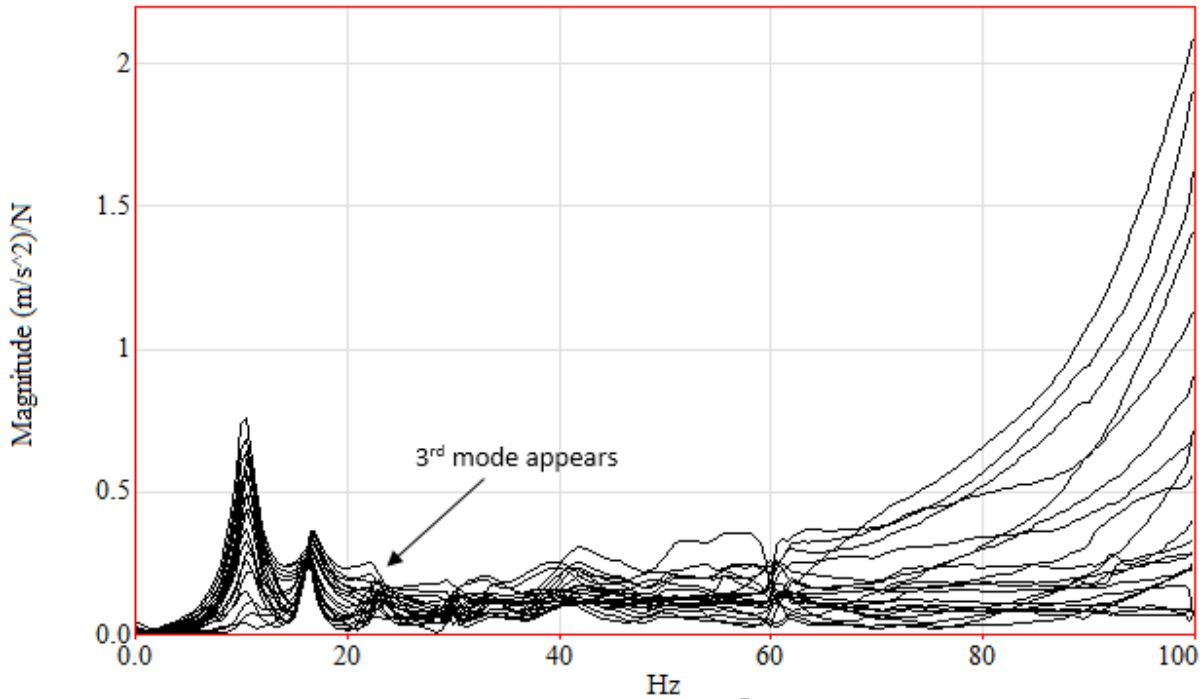


Fig. 15. FRFs estimation using phase controlled impact device for 30 Hz.

4.3. Comparison of modal extraction data

4.3.1. Running speed: 20 Hz

Comparison is made between these techniques at the same number of averages, i.e., 10 averages. This is to ensure that under the same averaging parameter, with different experimental conditions, i.e., static and operating condition, ISTA using phase controlled impact device is still able to achieve better performance and good agreement with respect to the classical method. Next, modal parameters are extracted from the FRFs estimation described in Section 4.2.1. An experimental benchmark data is obtained during stationary condition and used for the comparison and validation of the effectiveness of using the different excitation strategies, and results are tabulated in Table 5. As can be seen, the first two natural modes are excited by both manual impact hammer and the phase controlled impact device. For the case of using manual impact hammer, the first two modes are estimated at 10.7 Hz and 16.5 Hz respectively. However, the less sensitive third natural mode is covered up by the dominant cyclic load component at 20 Hz and thus is not successfully extracted. Meanwhile, the modal frequencies extracted from the estimated FRF using the phase controlled impact device are 10.5 Hz, 16.5 Hz and 22.9 Hz respectively.

A lower percentage difference in damping ratio is observed for phase controlled impact device for the first two natural modes in Table 5 compared to using manual impact hammer. The percentage difference between the benchmark and the phase controlled impact device in damping ratio estimates for the third natural mode is 15.83%. This is probably due to two reasons; (i) only 10 averages are used for modal testing using phase controlled impact device and thus, the disturbances could not be completely removed could cause error in the damping ratio estimates and (ii) damping ratio is estimated and compared under two different conditions, i.e., stationary and rotating condition. Note that the modal parameters of a system depending on three factors, i.e., geometry, material properties and boundary conditions. As the system is set to operate at 20 Hz, increases in vibration amplitude of the system possibly has led to boundary conditions change. Generally, the errors are small and it indicates a good suppression of the harmonic.

Table 5 has summarized the modal assurance criterion (MAC) values between the benchmark data and ISTA using manual impact hammer and phase controlled impact device to show the correlation of mode shapes. Both excitation strategies show high and stable MAC value for the first and second natural modes and these natural modes are far from the dominant cyclic load component of 20 Hz. The third natural mode could be estimated when the phase controlled impact device is used. The correlation of the mode shape with the benchmark data was high with a MAC value of 0.964 whereas for ISTA using manual impact hammer, the MAC value could not be identified.

Table 5

Summary of modal Parameter extraction based on FRFs from a benchmark (BM) measurement without the harmonic and ISTA using (A) Manual Impact Hammer and (B) phase controlled impact device for 20 Hz.

Mode	Natural frequency (Hz)			Damping ratio			Percentage of difference (%)				MAC	
							Natural frequency (Hz)		Damping ratio			
	BM	A	B	BM	A	B	BM vs. A	BM vs. B	BM vs. A	BM vs. B	BM vs. A	BM vs. B
1	10.	10.	10.	0.08	0.07	0.08	1.83	3.67	5.03	3.71	0.98	0.98
	9	7	5	35	93	66					3	8
2	16.	16.	16.	0.03	0.04	0.04	0.60	0.60	25.4	23.93	0.96	0.97
	6	5	5	97	98	92			4		4	6
3	22.	N/	22.	0.04	N/A	0.04	N/A	0	N/A	15.83	N/A	0.96

9	A	9	17	83	4
---	---	---	----	----	---

4.3.2. Running speed: 30 Hz

The modal extraction data are tabulated in Table 6. For ISTA using manual impact hammer, the first two natural frequencies identified are 10.6 Hz and 16.3 Hz whereas the third natural could not be identified as it is covered up by the dominant cyclic load component. In addition, the first three natural frequencies identified for ISTA using phase controlled impact device are 10.4 Hz, 16.4 Hz and 22.8 Hz. Generally, the percentage of difference is less than 5% for both excitation strategies. Owing to the fact that the first and second natural mode are far away from the excitation frequency, the MAC value for this natural modes are above 0.9 showing good correlation with the benchmark EMA. Moreover, elimination of the disturbances for ISTA using phase controlled impact device has led to the successful extraction of the less sensitive third natural mode with a MAC value of 0.980. Again, the highest percentage of difference for damping ratio registered at 14.86% for second natural mode as tabulated in Table 6. This is probably because there is still presence of small of amount disturbances as completely removal of disturbances may require more number of averages. Also, it is known that the dynamic characteristics of a system are governed by the geometric, material and boundary properties of the system. In this case, a slight changes in boundary conditions is possible as the vibration level of the system increases due the amplified rotational or imbalance force during operation especially the operating speed at 30 Hz. It is noticed that the errors are small and it indicates a good suppression of the cyclic load component and its harmonic.

Table 6

Summary of modal parameter extraction based on FRFs from a benchmark (BM) measurement without the harmonic and ISTA using (A) manual impact hammer and (B) phase controlled impact device for 30 Hz.

Mode	Natural frequency (Hz)			Damping ratio			Percentage of difference (%)				MAC	
							Natural frequency (Hz)		Damping ratio			
	BM	A	B	BM vs. A	BM vs. B	BM vs. A	BM vs. B	BM vs. A	BM vs. B			
1	10.	10.	10.	0.08	0.09	0.08	2.75	4.59	15.45	0.24	0.96	0.98
	9	6	4	35	64	37					5	8
2	16.	16.	16.	0.03	0.04	0.04	1.81	1.20	2.27	14.8	0.99	0.97

	6	3	4	97	06	56				6	0	0
3	22.	N/	22.	0.04	N/A	0.04	N/A	0.44	N/A	6.24	N/A	0.98
	9	A	8	17		43						0

As a whole, by using the phase controlled impact device as the excitation device in ISTA, users will have control over the impacts event as discussed in Section 4.1. The study has shown that with 10 and 20 averages are sufficient to eliminate the disturbances as the phase of the disturbances is always changing, (i.e. 180° difference for the case of 20 Hz and 90° for the case of 30 Hz) with respect to the impact. In this study, some deviations are observed in the natural frequencies and damping ratio obtained and this may be due to some changes in boundary condition, especially measurements are done during operating condition, causing the stiffness of the test rig to decrease. However, this is always the case when performing operational modal testing. In fact, the data obtained could better reflect the true dynamic characteristics of a system under actual boundary conditions during operating condition. Furthermore, a slight drop of MAC values is seen but it is crucial to remember that as long as the values are larger than 0.9, the results are indicating highly consistent mode shapes (21).

In general, the modal testing procedure during operation is thus enhanced in a way that; (i) a better FRF estimation with high signal to noise ratio (SNR) is obtained by the appearance of the third natural mode for both 20 Hz and 30 Hz; (ii) a percentage reduction of 87.96% cyclic load component at the maximum peak of 20 Hz, 91.65% at the maximum peak of 30 Hz and 59.03% at its second harmonic, 60 Hz; (iii) minimal number of averages/impacts applied has relatively expedited the modal testing procedure; (iv) improved and higher MAC value at running speed of 20 Hz and 30 Hz and (v) overall well correlation with the benchmark data.

4.4. Overall performance comparison with previous work and classical EMA during operating condition

To make a claim on this technique, it is useful to compare the overall performance of ISTA using the phase controlled impact device with previous literature as shown in Table 7. A ranking analysis using simple codes such as 0 for “same as”, - for “worse than” and + for “better than” has been performed. The reference here is ISTA using manual impact hammer due to the fact that the concept is proven from the previous literature. Several criteria are chosen for comparison in order to select, or adapt, the most suitable technique for operational modal testing.

In (19), four scenarios were presented with ISTA using manual impact hammer and it was reported that synchronization of between periodic response from cyclic load component and response due to impacts was still possible because each impact was applied at random instance or the impact

frequency is an integer multiples of the operating frequency. Thus, ISTA using phase controlled impact device scores a “+” because each impact can be applied at a correct time/phase and is always not synchronize with the disturbances. Besides, impact force level is another concern while performing ISMA in the presence of dominant periodic response from cyclic load component. For instance, if the excitation force is lower than the cyclic force, the FRFs estimation obtained could be severely affected by the disturbances and subsequent modal parameters identification are difficult (22). With phase controlled impact device, an adjustable input force level can guarantee each impact has sufficient force to excite the natural modes of interest.

Previous work has shown that well correlation with the benchmark EMA can be achieved if and only if high number of averages is considered when using impact hammer, i.e., 250 averages (23). The experimental testing can become very time-consuming; therefore phase controlled impact device using feedforward control approach can be implemented as elaborated in this study in the effort of reducing the disturbances with minimal averages while enhancing the FRFs estimation. “-” scores are given to EMA in FRFs estimation and signal to noise ratio criteria as the technique is not applicable for operational modal testing due to the fact that increasing number of averages (>250 averages) will not reduce the disturbances.

Since classical EMA is normally performed with fewer number of averages, the technique scores a “+” when compared to ISTA using manual impact hammer for man power criteria. The same score is given to ISTA using phase controlled impact device as the study has shown that 20 averages are sufficient to have excellent results, which is 12.5 times lesser from previous literature. However, ISTA using phase controlled impact device requires two additional hardware, i.e., DC power supply to power up the phase controlled impact device and tachometer for measuring disturbances. This explains why there are “-” scores in the equipment criteria compared to other two techniques. Lastly, double impacts and overload are often the sources of human error in vibration measurement when using manual impact hammer and these errors can be easily overcome with phase controlled impact device.

From the net score obtained, it is notable that ISTA using phase controlled impact device has more advantages than ISTA using manual impact hammer and classical EMA. The conclusion here is that EMA only limited to static condition and it is impractical to shut down the operating machine in today's high-technology petrochemical plants just to perform EMA as the cost of system downtime is very high. For that reason, ISTA using manual impact hammer was introduced previously but the procedure requires high number of averages which in turn may increase human errors and analysis time. Thus, ISTA using phase controlled impact device is seen to be a very good solution for the problem discussed.

Table 7

Ranking analysis between EMA and ISTA using manual impact hammer and phase controlled impact device during operating condition.

Criteria	EMA	ISTA using manual impact hammer	ISTA using phase controlled impact device
Synchronization of the impact with cyclic load	0	0	+
Impact condition			
a. Random impacts	0	0	+
b. Impact frequency	0	0	+
c. Impact force level	0	0	+
Number of averages required	+	0	+
FRFs estimation	-	0	+
Signal to noise ratio	-	0	+
Man power	+	0	+
Equipment:			
a. Cost	0	0	-
b. Set-up	0	0	-
Human error:			
a. Double impact	0	0	+
b. Overload	0	0	+
Sum +’s	2	0	10
Sum 0’s	8	12	0
Sum -’s	2	0	2
Net score	0	0	8
Rank	2	2	1

5. Conclusions

As stated before, lack of knowledge and control of impact with respect to the phase angle of the disturbances using conventional impact hammer in ISMA has limited the effectiveness and practicality of this novel technique. Therefore, a phase controlled impact device is introduced in this paper in the effort to eliminate non-synchronous components with a minimal number of averages by feeding the phase angle information of responses from the cyclic load back to the device. It utilizes the phase angle information and able to impart the impact at the correct time/phase which is always asynchronous with respect to the phase of response from cyclic load. The enhancement of the effectiveness of ISTA is shown by comparing the FRFs estimation obtained through two excitation strategies, i.e., manual impact hammer and phase controlled impact device. Results showed that a cleaner FRF estimation is obtained

using the phase controlled impact device, making it possible to estimate a third natural mode which is covered up by the dominant cyclic load component for ISTA using manual impact hammer. The percentage of reduction of disturbances can achieve 50-92%. Enhanced FRF estimation for ISTA using phase controlled impact device has led to more accurate modal parameters extraction where the first three natural modes are successfully determined and reveal a good correlation with the benchmark data. This is shown by the relatively low percentage of difference in natural frequency and MAC values between, i.e., 0.964-0.988 for 20 Hz and 0.988-0.970 for 30 Hz. Therefore, ISTA using phase controlled impact device has proven to be able to deliver highly accurate result which is suitable for modal testing during operation. It is a viable option for conventional method using manual impact hammer as the modal testing procedure can be more precise, faster and more efficient.

Acknowledgements

The authors wish to acknowledge the financial support and advice given by University of Malaya Research Grant (RP022D-2013AET), Fundamental Research Grant Scheme (FP010-2014A), Postgraduate Research Grant (PG011-2015A), Advanced Shock and Vibration Research (ASVR) Group of University of Malaya and other project collaborators.

References

- [1] T.T. William, & Marie, D. D, Theory of vibration with applications, 5 ed., New Jersey: Prentice Hall, 1998.
- [2] A. Brandt, Noise and Vibration Analysis: Signal Analysis and Experimental Procedures, Wiley, 2011.
- [3] P. Avitabile, Experimental modal analysis - A simple non-mathematical presentation, Sound Vib, 35 (2001) 20-31.
- [4] M.M. Fayyadh, H.A. Razak, Damage Identification and Assessment in Rc Structures Using Vibration Data: A Review, J Civ Eng Manag, 19 (2013) 375-386.
- [5] S.K. Loh, W.F. Farris, M. Hamdi, W.M. Chin, Vibrational characteristics of piping system in air conditioning outdoor unit, Sci China Technol Sc, 54 (2011) 1154-1168.
- [6] J. He, Z.-F. Fu, 1 - Overview of modal analysis, in: Modal Analysis, Butterworth-Heinemann, Oxford, 2001, pp. 1-11.
- [7] L. Zhang, T. Wang, Y. Tamura, A frequency-spatial domain decomposition (FSDD) method for operational modal analysis, Mechanical Systems and Signal Processing, 24 (2010) 1227-1239.
- [8] L. Hermans, H. Van der Auweraer, Modal testing and analysis of structures under operational conditions: Industrial applications, Mechanical Systems and Signal Processing, 13 (1999) 193-216.
- [9] M. Drusa, R.R. Nikolic, M. Marschalko, J. Grosel, W. Sawicki, W. Pakos, XXIII R-S-P Seminar, Theoretical Foundation of Civil Engineering (23RSP) (TFoCE 2014) Application of Classical and Operational Modal Analysis for Examination of Engineering Structures, Procedia Engineering, 91 (2014) 136-141.
- [10] D. Brown, R. Allemang, R. Zimmerman, M. Mergeay, Parameter estimation techniques for modal analysis, in, SAE Technical paper, 1979.

- [11] R.J. Allemang, D.L. Brown, A unified matrix polynomial approach to modal identification, *J Sound Vib*, 211 (1998) 301-322.
- [12] A.G.A. Rahman, Z.C. Ong, Z. Ismail, Enhancement of coherence functions using time signals in Modal Analysis, *Measurement*, 44 (2011) 2112-2123.
- [13] P. Mohanty, D.J. Rixen, Operational modal analysis in the presence of harmonic excitation, *J Sound Vib*, 270 (2004) 93-109.
- [14] E. Parloo, P. Verboven, P. Guillaume, M. Van Overmeire, Force identification by means of in-operation modal models, *J Sound Vib*, 262 (2003) 161-173.
- [15] Z.C. Ong, Development of impact-synchronous modal analysis technique on motor-driven structure during operation in: Department of Mechanical Engineering, University of Malaya, 2013.
- [16] A. Rahman, Z. Ismail, S. Noroozi, Z. Ong, Enhancement of Impact-synchronous Modal Analysis with number of averages, *J Vib Control*, 20 (2013) 1645-1655.
- [17] A.G.A. Rahman, et al., Impact-Synchronous Modal Analysis (ISMA)- An Attempt to Find an Alternative, in: 5th International Operational Modal Analysis Conference, Guimarães - Portugal, 2013.
- [18] A.G.A. Rahman, O.Z. Chao, Z. Ismail, Effectiveness of Impact-Synchronous Time Averaging in determination of dynamic characteristics of a rotor dynamic system, *Measurement*, 44 (2011) 34-45.
- [19] Z.C. Ong, H.C. Lim, S.Y. Khoo, Z. Ismail, K.K. Kong, A.G.A. Rahman, Assessment of the phase synchronization effect in modal testing during operation, *J Zhejiang Univ-Sc A*, 18 (2017) 92-105.
- [20] O.Z. Chao, M.A.M.A. Kor, A. Brandt, Experimental Validation of Phase Synchronisation Effects in Optimising Impact-Synchronous Time Averaging, in: 6th Iomac: International Operational Modal Analysis Conference Proceedings, 2015, pp. 629-636.
- [21] M. Pastor, M. Binda, T. Harcarik, Modal Assurance Criterion, *Modelling of Mechanical and Mechatronics Systems*, 48 (2012) 543-548.
- [22] O.Z. Chao, L.H. Cheet, K.S. Yee, A.G.A. Rahman, Z. Ismail, An experimental investigation on the effects of exponential window and impact force level on harmonic reduction in impact-synchronous modal analysis, *J Mech Sci Technol*, 30 (2016) 3523-3532.
- [23] A.G.A. Rahman, Z. Ismail, S. Noroozi, Z.C. Ong, Enhancement of Impact-synchronous Modal Analysis with number of averages, *J Vib Control*, 20 (2014) 1645-1655.